AMERICAN SOCIETY FOR MICROBIOLOGY | Molecular and Cellular Biology®

RESEARCH ARTICLE

Regulation of Intestinal Epithelial Barrier Function by Long Noncoding RNA *uc.173* through Interaction with MicroRNA 29b

Jun-Yao Wang,[a,b]* Yu-Hong Cui,[a,b]* Lan Xiao,[a,b] Hee Kyoung Chung,[a,b] Yunzhan Zhang,[a,b] Jaladanki N. Rao,[a,b] Myriam Gorospe,[c] Jian-Ying Wang[a,b,d]

[a]Cell Biology Group, Department of Surgery, University of Maryland School of Medicine, Baltimore, Maryland, USA

[b]Baltimore Veterans Affairs Medical Center, Baltimore, Maryland, USA

[c]Laboratory of Genetics and Genomics, National Institute on Aging Intramural Research Program, NIH, Baltimore, Maryland, USA

[d]Department of Pathology, University of Maryland School of Medicine, Baltimore, Maryland, USA

ABSTRACT The mammalian intestinal epithelium establishes a selectively permeable barrier that supports nutrient absorption and prevents intrusion by noxious luminal substances and microbiota. The effectiveness and integrity of the barrier function are tightly regulated via well-controlled mechanisms. Long noncoding RNAs transcribed from ultraconserved regions (T-UCRs) control diverse cellular processes, but their roles in the regulation of gut permeability remain largely unknown. Here we report that the T-UCR *uc.173* enhances intestinal epithelial barrier function by antagonizing microRNA 29b (miR-29b). Decreasing the levels of *uc.173* by gene silencing led to dysfunction of the intestinal epithelial barrier in cultured cells and increased the vulnerability of the gut barrier to septic stress in mice. *uc.173* specifically stimulated translation of the tight junction (TJ) claudin-1 (CLDN1) by associating with miR-29b rather than by binding directly to *CLDN1* mRNA. *uc.173* acted as a natural decoy RNA for miR-29b, which interacts with *CLDN1* mRNA via the 3′ untranslated region and represses its translation. Ectopically expressed *uc.173* abolished the association of miR-29b with *CLDN1* mRNA and restored claudin-1 expression to normal levels in cells overexpressing miR-29b, thus rescuing the barrier function. These results highlight a novel function of *uc.173* in controlling gut permeability and define a mechanism by which *uc.173* stimulates claudin-1 translation, by decreasing the availability of miR-29b to *CLDN1* mRNA.

KEYWORDS T-UCRs, microRNA, posttranscriptional regulation, gut permeability, tight junction, septic stress

The mammalian intestinal epithelial barrier depends on specialized structures named tight junctions (TJs) and adherens junctions (AJs) that protect the subepithelial tissue against a wide array of luminal noxious substances, allergens, and microbial pathogens (1, 2). TJs are located at the apical region of the epithelial lateral membrane and fence the paracellular space in the intestinal epithelium, which is selectively permeable to certain hydrophilic molecules, ions, and nutrients (1, 3). Functional TJ complexes in the epithelium primarily include TJ-transmembrane proteins, such as the claudin family of proteins, which interact directly with a cytosolic plaque of TJ-membrane-associated proteins, such as ZO-1, that bind to the cortical cytoskeleton (3, 4). Immediately below the TJs are the cadherin-rich AJs, which mediate strong cell-to-cell adhesion and also integrate distinct cellular signals to regulate epithelial paracellular permeability (5). Both TJ and AJ complexes are highly dynamic, and their constituent proteins undergo continuous remodeling and turnover (1, 6, 7). Maintenance of dynamic levels of TJ and AJ proteins is essential for the integrity of the epithelial barrier function, a process that is tightly controlled by numerous extracellular and intracellular

Received 8 January 2018 **Returned for modification** 4 February 2018 **Accepted** 2 April 2018

Accepted manuscript posted online 9 April 2018

Citation Wang J-Y, Cui Y-H, Xiao L, Chung HK, Zhang Y, Rao JN, Gorospe M, Wang J-Y. 2018. Regulation of intestinal epithelial barrier function by long noncoding RNA *uc.173* through interaction with microRNA 29b. Mol Cell Biol 38:e00010-18. https://doi.org/10.1128/MCB.00010-18.

Address correspondence to Jian-Ying Wang, jywang@som.umaryland.edu.

* Present address: Jun-Yao Wang, Department of Gastroenterology, People's Hospital, Peking University School of Medicine, Beijing, People's Republic of China; Yu-Hong Cui, Department of Histology and Embryology, Guangzhou Medical University, Guangzhou, Guangdong, People's Republic of China.

factors (5, 8). Acute epithelial barrier dysfunction occurs commonly in various critical pathological conditions, leading to the translocation of luminal toxic substances and bacteria to the bloodstream and, in some instances, to multiple organ dysfunction syndrome and death (9), but the mechanisms responsible for this dysfunction are largely unknown.

The human genome transcribes a large number of noncoding RNAs (ncRNAs), such as microRNAs (miRNAs), endogenous small interfering RNAs (siRNAs), natural antisense transcripts (NATs), and long noncoding RNAs (lncRNAs), while protein-coding transcripts account for only a minority of the transcriptional output (10, 11). lncRNAs, defined as being at least 200 nucleotides long, have recently attracted much attention due to their abundant presence in the human genome, tissue-specific expression patterns in response to stress, and functional relevance in complex physiologic processes and pathological conditions (12, 13). lncRNAs can create complex regulatory networks by interacting with different molecular partners, such as transcription factors, histones or other chromatin-modifying proteins, and RNA-binding proteins (RBPs), to regulate gene expression at multiple levels (12, 14). Emerging evidence also shows that the interplay between lncRNAs and miRNAs controls gene regulatory programs involved in many aspects of cellular processes and human diseases (12, 15, 16). In this regard, lncRNAs can be primary miRNAs (pri-miRNAs) (15), act as molecular sponges for miRNAs (16), and regulate miRNA processing (17). Recently, lncRNA *H19* was found to disrupt the intestinal epithelial barrier by serving as a precursor for miRNA 675 (miR-675) (18), whereas lncRNA *SPRY4-IT1* enhanced intestinal epithelial barrier function by increasing the expression of TJs at the posttranscription level via interaction with RBP HuR (19, 20).

Ultraconserved regions (UCRs) are sequences located in both intra- and intergenic regions that are absolutely conserved (100%) among the orthologous regions of the human, rat, and mouse genomes (21). Although UCRs are actively transcribed in various tissues, more than half of all 481 known UCRs have no protein-coding potential. RNAs transcribed from these UCRs (T-UCRs) have been identified as a class of novel lncRNAs that regulate proliferation and apoptosis (22–24). The expression levels of T-UCRs are altered in response to stress conditions and pathologies. For example, the levels of cellular *uc.349A*, *uc.352*, *uc.338*, *uc.8*, *uc.339*, *uc.63+*, and *uc.475* (22–28) increased dramatically in human cancers or after exposure to hypoxia. We have reported that 21 T-UCRs, including *uc.173*, are differentially expressed in the intestinal mucosae of fasted mice relative to expression in nonfasted mice and that increasing the levels of *uc.173* promotes mucosal renewal of the intestine by inducing the degradation of pri-miR-195 (29). In this study, we investigate the role of *uc.173* in the regulation of the intestinal epithelial barrier and present evidence that *uc.173* stimulates the translation of TJ claudin-1 (CLDN1) through interaction with miR-29b, thus enhancing epithelial barrier function.

RESULTS

***uc.173* silencing leads to intestinal epithelial barrier dysfunction *in vitro*.** To investigate the role of *uc.173* in the regulation of the intestinal epithelial barrier function, we silenced the expression of *uc.173* by transfecting human epithelial colorectal adenocarcinoma Caco-2 cells with locked nucleic acid (LNA)-modified anti-uc.173 oligonucleotides (anti-uc.173). As shown in Fig. 1A (left), levels of cellular *uc.173* were dramatically lower in cells transfected with LNA-modified anti-uc.173 than in cells transfected with control oligonucleotides (Con-oligo). This effect of anti-uc.173–LNA was specific, as evidenced by the fact that it did not alter the abundance of T-UCR *uc.346* (Fig. 1A, right). Decreasing the levels of *uc.173* by anti-uc.173 transfection specifically inhibited expression of the TJ claudin-1 but failed to alter cellular levels of other TJs, such as claudin-3, occludin, JAM-1, and ZO-1, the AJ E-cadherin, and UBE2B protein (the product of the *uc.173* host gene) (Fig. 1B). The levels of claudin-1 protein in a population of cells in which *uc.173* was silenced decreased by ~75% ($n = 3$) ($P < 0.05$) from those in cells transfected with control oligonucleotides. In accordance with this result, immunostaining also revealed that claudin-1 protein levels decreased

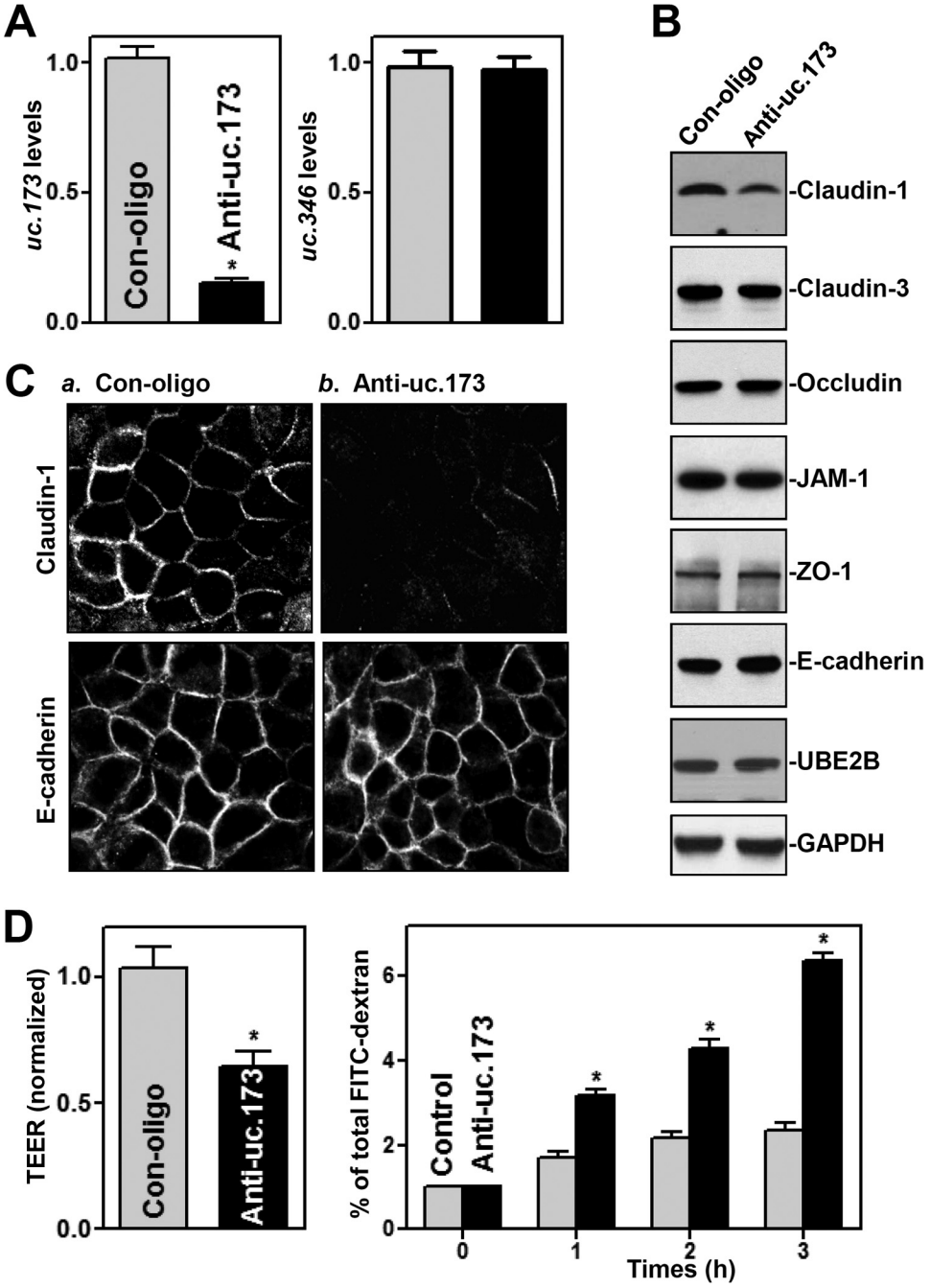

FIG 1 LNA-mediated *uc.173* silencing inhibits claudin-1 expression and disrupts epithelial barrier function. (A) Levels of cellular *uc.173* 48 h after transfection with LNA-siRNA targeting *uc.173* (anti-uc.173) or a control siRNA (Con-oligo) in Caco-2 cells. Values are relative to control levels and are means ± SEM from triplicate experiments. The asterisk indicates a significant difference ($P < 0.05$) from the Con-oligo result. (B) Representative immunoblots of tight junctions and an adherens junction in cells treated as described for panel A. Three experiments were performed, with similar results. (C) Distribution of claudin-1 and E-cadherin in cells treated as described for panel A. Forty-eight hours after transfection, cells were fixed, permeabilized, and incubated first with an antibody against claudin-1 or E-cadherin and then with FITC-conjugated anti-IgG. Original magnification, ×500. (D) Changes in epithelial barrier function, as indicated by changes in TEER (left) and FITC-dextran paracellular permeability (right), in cells treated as described for panel A. TEER assays were performed on 12-mm Transwell filters; paracellular permeability was assayed by adding the membrane-impermeant trace molecule FITC-dextran to the insert medium. Values are means ± SEM of data from six samples. Asterisks indicate significant differences ($P < 0.05$) from the Con-oligo results.

remarkably after *uc.173* silencing (Fig. 1C, top), although there were no differences in the extent of immunostaining of E-cadherin between anti-uc.173-transfected cells and cells transfected with control oligonucleotides (Fig. 1C, bottom).

Importantly, *uc.173* silencing disrupted epithelial barrier function in an *in vitro* model, as evidenced by a decrease in transepithelial electrical resistance (TEER) values (Fig. 1D, left) and an increase in the levels of paracellular flux of fluorescein isothiocyanate (FITC)-dextran (Fig. 1D, right). To exclude off-target effects, other LNA-modified anti-uc.173 oligonucleotides were tested; a similar repressive effect was observed on the expression of *uc.173*, as well as on claudin-1 expression levels and epithelial barrier function (data not shown). Transfection with either anti-uc.173 or control oligonucleotides did not affect cell viability, as examined by trypan blue staining (data not shown). These data indicate that the T-UCR *uc.173* is essential for normal expression of the TJ claudin-1 and for the maintenance of epithelial barrier function *in vitro*.

***uc.173* enhances the translation of claudin-1.** To examine the effect of increasing the levels of *uc.173* on claudin-1 expression, Caco-2 cells were transfected with a plasmid vector expressing *uc.173* under the control of the cytomegalovirus (CMV) promoter, as described in our previous study (29). As shown in Fig. 2A, the abundance of *uc.173* increased substantially by 48 h after transfection, but that of *uc.346* did not. Ectopically expressed *uc.173* specifically stimulated the expression of claudin-1, with no effect on the expression levels of the claudin-3, occludin, JAM-1, ZO-1, E-cadherin, and UBE2B proteins (Fig. 2B).

To investigate the mechanism underlying the stimulation of claudin-1 expression by *uc.173*, we examined the changes in *CLDN1* mRNA levels and found that neither the silencing nor the overexpression of *uc.173* altered the content of *CLDN1* mRNA (see Fig. S1 in the supplemental material), suggesting that *uc.173* might regulate claudin-1 expression at the translational level. To test this possibility, we examined the rate of *CLDN1* mRNA translation by use of the Click-iT technology (see Materials and Methods) as described previously (18). The levels of newly synthesized claudin-1 protein in cells overexpressing *uc.173* were significantly higher than those in cells transfected with a control vector (Fig. 2C). The stimulation of claudin-1 protein synthesis by *uc.173* was specific, since there were no changes in the levels of nascent glyceraldehyde-3-phosphate dehydrogenase (GAPDH) synthesis after transfection with the *uc.173* expression vector.

To further investigate the role of *uc.173* in the regulation of claudin-1 translation, we measured the relative distribution of *CLDN1* mRNA in individual fractions from polyribosome gradients after ectopic overexpression of *uc.173* as reported previously (30). Although increasing the levels of *uc.173* did not affect global polysomal profiles (data not shown), the association of *CLDN1* mRNA with actively translating fractions (fractions 10 to 12) increased in cells overexpressing *uc.173*, along with a reduction in the levels of *CLDN1* mRNA in low-translating fractions (fractions 7 to 9) (Fig. 2D, left). In contrast, *GAPDH* mRNA, encoding a housekeeping protein, was distributed similarly in the two groups (Fig. 2D, right). These data reveal that *uc.173* stimulates claudin-1 translation without affecting *CLDN1* mRNA levels.

A reduction in *uc.173* abundance increases the vulnerability of the gut barrier to pathological stress. In an effort to define the *in vivo* function of *uc.173* in regulating gut permeability, the levels of endogenous *uc.173* in the intestinal mucosa were decreased by administering systemically the same LNA-modified anti-uc.173 oligonucleotides that were used in cultured intestinal epithelial cells (IECs). As reported in our previous study (29), treatment with anti-uc.173 for 4 consecutive days caused a sustained decrease in *uc.173* levels in the small intestinal mucosa (Fig. 3A, left) but did not alter the levels of *uc.346* (Fig. 3A, center) or *U6* (Fig. 3A, right) RNA. The levels of mucosal *uc.173* in the small intestine were ~70% lower in mice treated with anti-uc.173 than in animals treated with control oligonucleotides. In contrast to the findings observed *in vitro*, decreasing the levels of *uc.173* in the mucosa did not affect the basal

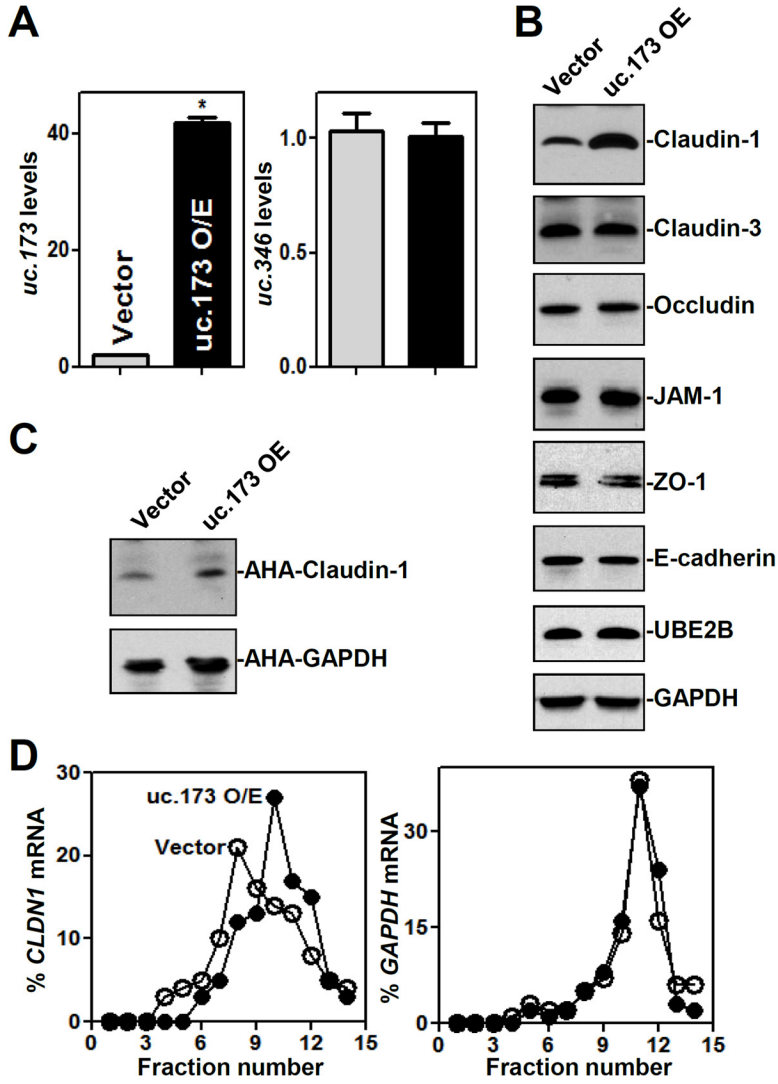

FIG 2 Ectopically expressed *uc.173* enhances claudin-1 translation. (A) Levels of *uc.173* (left) and *uc.346* (right) in cells transfected with the *uc.173* expression vector and measured 48 h later by RT-Q-PCR. Values are relative to those for the control (Vector) and are means ± SEM from triplicate experiments. O/E, overexpression. The asterisk indicates a significant difference ($P < 0.05$) from the result with the control vector. (B) Representative immunoblots of tight junctions and an adherens junction in cells treated as described for panel A. (C) Newly synthesized claudin-1 protein in cells treated as described for panel A. After cells were exposed to L-azidohomoalanine (AHA), cell lysates were incubated with the reaction buffer containing a biotin-alkyne reagent; the biotin-alkyne-azide-modified protein complex was pulled down by paramagnetic streptavidin-conjugated Dynabeads. (D) Distribution of *CLDN1* mRNA in each gradient fraction prepared from polysomal profiles in cells treated as described for panel A. Nuclei were pelleted, and the resulting supernatants were fractionated through a 10-to-50% linear sucrose gradient. Total RNA was isolated from different fractions, and the level of *CLDN1* or *GAPDH* mRNA in each fraction was measured and plotted as a percentage of the total level of *CLDN1* or *GAPDH* mRNA, respectively, in each sample.

level of gut permeability (Fig. 3B) in control mice (sham-treated groups), although the levels of claudin-1 protein decreased in anti-uc.173-treated mice (Fig. 3C).

To determine if a reduction in the abundance of *uc.173* in tissue affected the vulnerability of the gut barrier in critical pathological conditions, we subjected the mice to septic stress using the cecal ligation and puncture (CLP) model (31). Exposure to CLP for 24 h led to acute gut barrier dysfunction in both anti-uc.173-treated mice and mice treated with control oligonucleotides, as indicated by an increase in gut mucosal permeability to FITC-dextran. Of interest, however, the levels of increased gut permeability due to CLP in mice treated with anti-uc.173 were much higher than those in mice

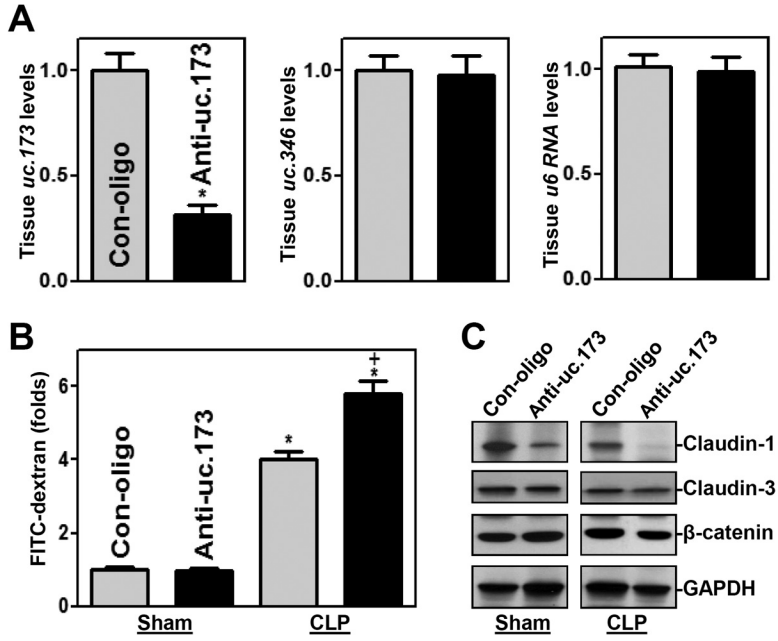

FIG 3 Inhibition of *uc.173* impairs gut barrier function in mice subjected to CLP. (A) Levels of *uc.173* (left), *uc.346* (center), and *U6* (right) RNAs in the small intestinal mucosae of mice injected intraperitoneally with LNA-modified anti-uc.173 or control oligonucleotides (Con-oligo) for 4 consecutive days. On day 5, total RNA was isolated for RT-Q-PCR analysis. Values are relative to those with Con-oligo and are means ± SEM of data from 5 animals. The asterisk indicates a significant difference ($P < 0.05$) from the Con-oligo result. (B) Gut permeability in sham-treated mice and in mice exposed to CLP for 24 h. FITC-dextran was given orally, and blood samples were collected 4 h later. The asterisk and plus sign indicate significant differences ($P < 0.05$) from sham-treated mice and from mice treated with Con-oligo and CLP, respectively. (C) Representative immunoblots of claudin-1, claudin-3, and β-catenin in the small intestinal mucosae of mice treated as described for panel B.

treated with control oligonucleotides (Fig. 3B). As expected, CLP stress decreased the levels of both claudin-1 and claudin-3 in the intestinal mucosa, but the inhibition of claudin-1 was amplified by decreasing the levels of *uc.173* in anti-uc.173-treated mice (Fig. 3C). In fact, claudin-1 protein disappeared almost completely in anti-uc.173-treated mice subjected to CLP. On the other hand, there were no significant changes in claudin-3 reduction (Fig. 3C) or in histological features of the small intestinal mucosa between mice treated with anti-uc.173 and mice treated with control oligonucleotides after CLP (data not shown). Additionally, treatment with either anti-uc.173 or control oligonucleotides for 4 consecutive days did not result in diarrhea, loss of body weight, loss of hair, or decreased activity in mice (data not shown). These results show that decreasing the levels of *uc.173* in the intestinal mucosa increases the vulnerability of the gut barrier to septic stress in mice.

***uc.173* does not bind to *CLDN1* mRNA but interacts directly with miR-29b.** To test if *uc.173* activates claudin-1 translation through direct interaction with *CLDN1* mRNA, we tagged *uc.173* with MS2 hairpins (Fig. 4A) and coexpressed it in cells along with the chimeric protein MS2–glutathione *S*-transferase (GST). After affinity purification using glutathione-SH beads, the RNAs present in the ribonucleoprotein complexes were examined by real-time quantitative PCR (Q-PCR) analysis as reported previously (32). Cells were cotransfected with the pMS2 (control) or pMS2-uc.173 vector along with pMS2-GST, and the binding of *uc.173* to *CLDN1* mRNA and miRNAs was examined 24 h after transfection. As shown in Fig. 4B, *uc.173* levels increased significantly. There were no differences in the levels of *CLDN1* mRNA in materials pulled down by MS2-GST between cells transfected with pMS2-uc.173 and cells transfected with pMS2 (Fig. 4C), indicating that *uc.173* does not bind directly to *CLDN1* mRNA. Because miR-29b is highly expressed in IECs and plays an important role in maintaining intestinal epithelial homeostasis (33–35), we examined the interaction of *uc.173* with miR-29b. Interestingly,

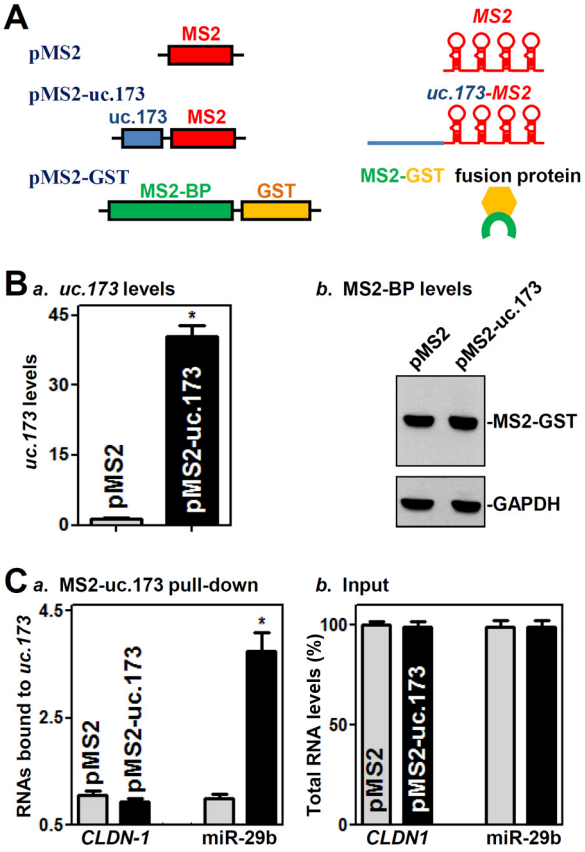

FIG 4 *uc.173* interacts with miR-29b but not with *CLDN1* mRNA. (A) Schematic of plasmids used for assays of *CLDN1* mRNA and miR-29b pulldown. pMS2 and pMS2-uc.173 expressed MS2 and MS2-*uc.173* RNAs, respectively, each containing 24 tandem MS2 hairpins; pMS2-GST expressed a fusion protein (MS2-GST) that can pull down MS2-containing RNA. (B) Levels of *uc.173* (a) and MS2-BP (b) 24 h after cotransfection with pMS2-GST and the pMS2 or pMS2-uc.173 vector. Values are relative to those with the pMS2 vector and are means ± SEM from triplicate experiments. The asterisk indicates a significant difference ($P < 0.05$) from the result for cells transfected with pMS2. (C) Binding of pMS2-uc.173 to RNAs. Shown are levels of *CLDN1* mRNA and miR-29b in the materials pulled down by pMS2-uc.173, given relative to levels with pMS2 (a) and as percentages of total input RNAs (b). The asterisk indicates a significant difference ($P < 0.05$) from the result for cells transfected with pMS2.

miR-29b levels were enriched in materials pulled down from cells transfected with pMS2-uc.173 relative to levels from cells transfected with pMS2 (Fig. 4Ca). The interaction of *uc.173* with miR-29b was specific, since increasing the amount of pMS2-uc.173 did not increase the level of miR-222 or lncRNA *H19* in the pulldown materials (see Fig. S2 in the supplemental material). In addition, cotransfection with pMS2-GST and pMS2 or pMS2-uc.173 did not alter the steady-state levels of *CLDN1* mRNA or miR-29b (Fig. 4Cb).

Since *uc.173* shows perfect complementarity with miR-29b at 8 nucleotides at its 3′ terminus (Fig. 5A), we investigated further the direct interaction between these two ncRNAs by using biotinylated miR-29b as described previously (19, 33). Twenty-four hours after transfection, miR-29b levels were significantly higher in cells transfected with biotin-labeled miR-29b than in cells transfected with a control scrambled oligomer (Fig. 5B, left), although the levels of *U6* RNA did not differ between these two groups (Fig. 5B, right). As expected, *uc.173* levels in samples pulled down using biotin-labeled miR-29b were much higher than those in samples pulled down using a biotin-labeled scrambled oligomer (Fig. 5Ca). Biotin-labeled miR-29b did not pull down other T-UCRs, such as *uc.346* and *uc.283*; transfection with biotin-labeled miR-29b also failed to alter the levels of input RNAs (Fig. 5Cb). These results strongly suggest that *uc.173* binds directly to miR-29b and can reduce the availability of miR-29b.

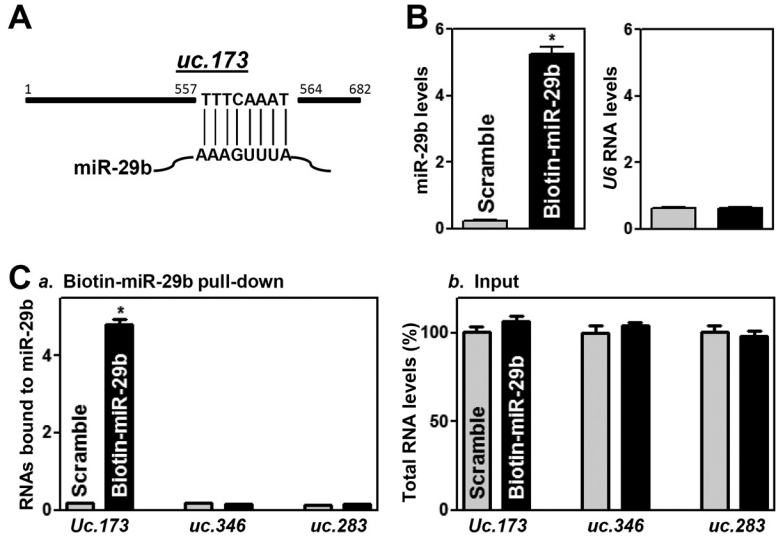

FIG 5 Biotinylated miR-29b associates with *uc.173*. (A) Schematic of *uc.173* depicting its complementarity with miR-29b. (B) Levels of biotinylated miR-29b (left) and *U6* RNA (right) 24 h after transfection with biotinylated miR-29b as measured by Q-PCR analysis. Values are relative to those with the scrambled oligonucleotide and are means ± SEM of data from triplicate experiments. The asterisk indicates a significant difference ($P < 0.05$) from the result for cells transfected with the control scrambled oligomer. (C) Binding of biotinylated miR-29b to T-UCRs. Shown are levels of *uc.173*, *uc.346*, and *uc.283* in the materials pulled down by biotin–miR-29b, given relative to the level with the scrambled oligomer (a) and as percentages of total input RNAs (b). The asterisk indicates a significant difference ($P < 0.05$) from the result for cells transfected with the scrambled oligonucleotide.

miR-29 interacts with *CLDN1* mRNA and represses its translation. *CLDN1* mRNA is a potential target of miR-29b, since there are two predicted binding sites for miR-29b within its 3′ untranslated region (3′ UTR) (Fig. 6A). Thus, we examined the association of miR-29b with *CLDN1* mRNA by RNA pulldown assays using biotin-labeled miR-29b (Fig. 6Ba). Twenty-four hours after transfection with biotin-labeled miR-29b (Fig. 6Bb), *CLDN1* mRNA was found to be enriched in materials pulled down by biotin–miR-29b but not in materials from cells transfected with a biotin-labeled control scrambled oligomer (Fig. 6Bc). On the other hand, biotin–miR-29b failed to pull down the mRNAs encoding E-cadherin and CUG-binding protein 1 (CUGBP1). To determine the functional consequence of miR-29b–*CLDN1* mRNA association, we examined whether increasing the levels of miR-29b through transfection with its precursor (pre-miR-29b) reduced the expression of claudin-1. Transient transfection with pre-miR-29b dramatically increased miR-29b levels (Fig. 6C, left), although it did not alter *U6* RNA levels (Fig. 6C, right). In contrast to the findings observed for cells overexpressing *uc.173*, increasing the levels of miR-29b by pre-miR-29b transfection specifically inhibited the expression of claudin-1 without affecting the expression levels of E-cadherin and β-catenin (Fig. 6D); *CLDN1* mRNA levels decreased by ~12% in cells transfected with pre-miR-29b, but this difference was not statistically significant. In turn, ectopically expressed miR-29b also resulted in epithelial barrier dysfunction, as revealed by a decrease in TEER values and an increase in paracellular permeability (see Fig. S3 in the supplemental material). Moreover, miR-29b overexpression inhibited claudin-1 expression predominantly by repressing its translation, since increasing the levels of miR-29b decreased the abundance of *CLDN1* mRNA in actively translating fractions of polyribosome gradients and showed a significant shift to weakly translating fractions (fractions 4 and 5) (Fig. 6E, left). In contrast, transfection with pre-miR-29b did not alter the distribution of *GAPDH* mRNA (Fig. 6E, right) or global polysomal profiles (data not shown).

To determine whether the repression of claudin-1 translation by miR-29b was mediated through the *CLDN1* 5′ UTR, coding region (CR), or 3′ UTR, fractions of the *CLDN1* 5′ UTR, CR, and 3′ UTR were subcloned into the Dual-Luciferase miRNA target expression vector pmirGLO to generate reporter constructs pmirGLO-CLDN1-5′UTR, pmirGLO-CLDN1-CR, and

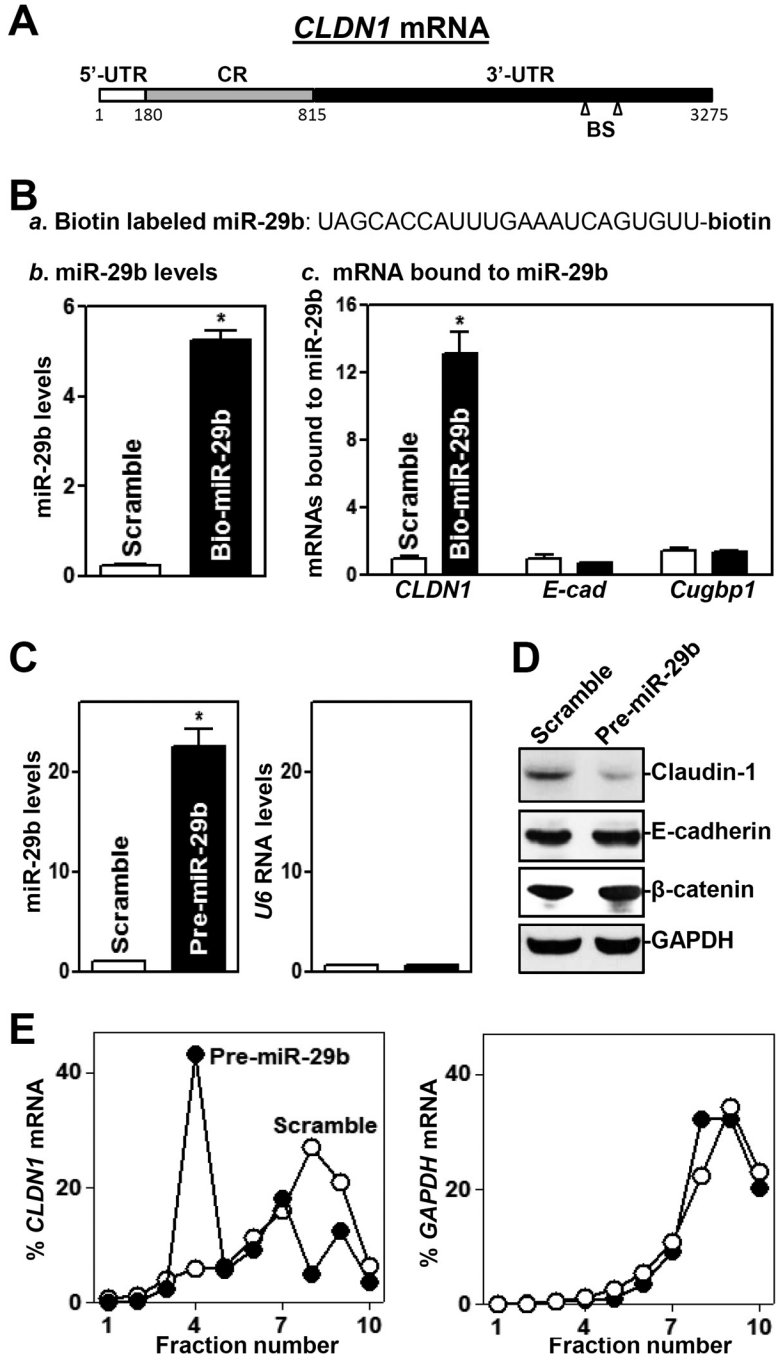

FIG 6 miR-29b represses claudin-1 translation. (A) Schematic representation of *CLDN1* mRNA depicting predicted target sites for miR-29b in its 3′ UTR. BS, predicted miR-29b-binding site. (B) Binding of biotinylated miR-29b to *CLDN1* mRNA. (a) Schematic representation of biotinylated miR-29b; (b) miR-29b levels 24 h after transfection; (c) levels of mRNAs encoding claudin-1, E-cadherin (*E-cad*), and CUG-binding protein 1 (*Cugbp1*) in materials pulled down by biotin–miR-29b. Values are relative to that with the control scrambled oligomer and are means ± SEM of data from triplicate experiments. The asterisk indicates a significant difference ($P < 0.05$) from the result for cells transfected with the control scrambled oligomer. (C) Levels of miR-29b in cells transfected with pre-miR-29b for 48 h. The asterisk indicates a significant difference ($P < 0.05$) from the result for cells transfected with the control scrambled oligomer. (D) Representative immunoblots of claudin-1, E-cadherin, and β-catenin in cells treated as described for panel C. (E) Distribution of *CLDN1* mRNA in each gradient fraction prepared from polysomal profiles in cells treated as described for panel C. The levels of *CLDN1* or *GAPDH* mRNAs were measured and plotted as percentages of total *CLDN1* or *GAPDH* mRNA levels in the samples, respectively.

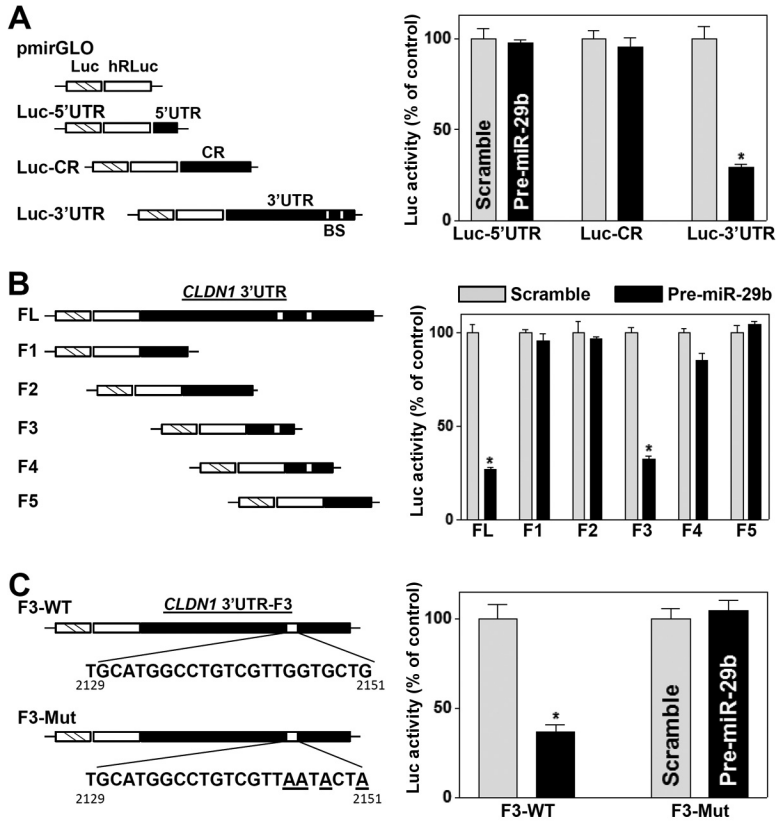

FIG 7 Deletion of the miR-29b binding site in the *CLDN1* 3′ UTR prevents miR-29b-mediated repression of claudin-1. (A) (Left) Schematic of *CLDN1* 5′ UTR, CR, and 3′ UTR luciferase (Luc) reporters. (Right) Levels of reporter activities after ectopic overexpression of miR-29b. BS, predicted miR-29b-binding site. Twenty-four hours after transfection with pre-miR-29b, cells were transfected with different *CLDN1* luciferase reporter plasmids. The levels of firefly and *Renilla* luciferase activities were assayed 24 h later. The results were normalized to *Renilla* luciferase activities and are expressed as means ± SEM of data from triplicate experiments. The asterisk indicates a significant difference ($P < 0.05$) from the result for cells transfected with the scrambled oligomer. (B) Effects of 5′ deletions of the *CLDN1* 3′ UTR (as shown in the schematic) on its luciferase reporter activity in cells treated as described for panel A. Asterisks indicate significant differences ($P < 0.05$) from results for cells transfected with the scrambled oligomer. (C) Effect of point mutation of a specific miR-29b binding site (schematic) in *CLDN1* 3′UTR-F3 on its luciferase reporter activity in cells treated as described for panel A. WT, wild type. The asterisk indicates a significant difference ($P < 0.05$) from the result for cells transfected with the scrambled oligomer.

pmirGLO-CLDN1-3′UTR (Fig. 7A, schematic). As shown in Fig. 7A (right), miR-29b overexpression by transfection with pre-miR-29b selectively decreased the level of CLDN1-3′UTR luciferase reporter activity but did not inhibit the activity of the CLDN1-5′UTR or -CR reporter, indicating that miR-29b inhibits claudin-1 translation through the *CLDN1* 3′ UTR. To further characterize the specific binding site of miR-29b in the *CLDN1* 3′ UTR, we prepared various reporter constructs that expressed chimeric RNAs containing the luciferase and a partial *CLDN1* 3′ UTR with or without the potential binding site (Fig. 7B, schematic). Ectopic miR-29b overexpression decreased the levels of luciferase reporter gene activity when cells were transfected with the full-length 3′ UTR (3′UTR-FL) or with a construct containing the miR-29b binding site located at positions 2129 to 2151 (3′UTR-F3) but not when cells were transfected with 3′UTR-F1, -F2, -F4 (which also contains a predicted binding site), or -F5 (Fig. 7B, right).

To gain a more detailed understanding of this regulatory paradigm, four nucleotides of *CLDN1* 3′UTR-F3, located at the F3 site of the *CLDN1* 3′ UTR, were mutated (Fig. 7C, schematic). As shown in Fig. 7C (right), repression of claudin-1 by miR-29b was completely prevented when this specific site from the *CLDN1* 3′ UTR was mutated. These results indicate that miR-29b interacts with *CLDN1* mRNA via the specific binding site at positions 2129 to 2151, thereby repressing claudin-1 translation.

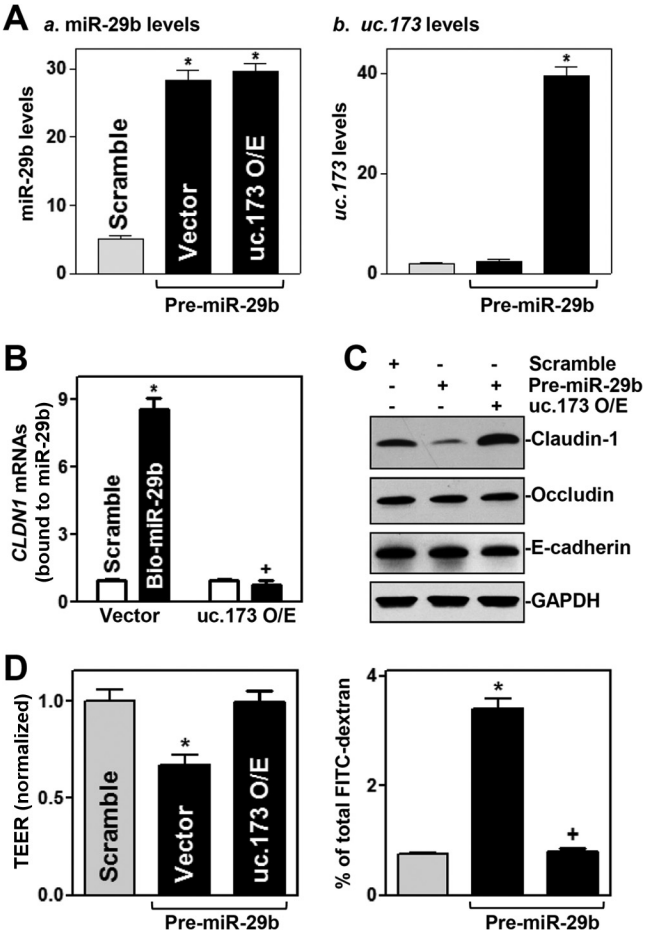

FIG 8 Ectopically expressed *uc.173* prevents miR-29b-induced epithelial barrier dysfunction. (A) Levels of miR-29b (a) and *uc.173* (b) 48 h after cells were either transfected with pre-miR-29b alone or cotransfected with pre-miR-29b and a *uc.173* expression vector. O/E, overexpression. Values are relative to those with a scrambled control oligomer and are means ± SEM of data from triplicate experiments. Asterisks indicate significant differences ($P < 0.05$) from results for cells transfected with the scrambled oligomer. (B) Effect of increasing *uc.173* levels on the association of miR-29b with *CLDN1* mRNA. Twenty-four hours after cells were transfected with a *uc.173* expression vector, they were transfected with biotin-labeled miR-29b (Bio-miR-29b). The levels of *CLDN1* mRNA in the materials pulled down by miR-29b were examined 24 h thereafter. The asterisk and plus sign indicate significant differences ($P < 0.05$) from the results for cells transfected with a scrambled oligomer or for cells transfected with Bio-miR-29b and a control vector, respectively. (C) Representative immunoblots of claudin-1, occludin, and E-cadherin proteins in cells treated as described for panel A. (D) Changes in TEER (left) and FITC-dextran paracellular permeability (right) in cells treated as described for panel A. Values are means ± SEM of data from six samples. The asterisks and plus sign indicate significant differences ($P < 0.05$) from results for cells transfected with a scrambled oligomer or with pre-miR-29b alone, respectively.

Elevation of *uc.173* expression prevents miR-29b-induced epithelial barrier dysfunction. To test the possibility that *uc.173* stimulates claudin-1 translation by decreasing the association of miR-29b with *CLDN1* mRNA, we cotransfected cells with pre-miR-29b and a *uc.173* expression vector. As shown in Fig. 8A, increasing the levels of *uc.173* did not affect induced miR-29b levels in cells cotransfected with pre-miR29b and the *uc.173* expression vector. However, increased *uc.173* levels abolished the binding of miR-29b to *CLDN1* mRNA. There were no differences in the levels of *CLDN1* mRNA in pulldown materials between cells transfected with biotin-labeled miR-29b and cells transfected with a biotin-labeled control scrambled oligomer after *uc.173* overexpression (Fig. 8B). Cotransfection with biotin-labeled miR-29b and the *uc.173* expression vector did not affect the total input of *CLDN1* mRNA (see Fig. S4 in the supplemental material). In accordance with this effect, elevation of *uc.173* expression also prevented the inhibition of claudin-1 expression (Fig. 8C) and restored epithelial barrier function

(Fig. 8D) in cells overexpressing miR-29b. The levels of TEER and FITC-dextran flux in cells cotransfected with pre-miR-29b and the *uc.173* expression vector were indistinguishable from those in cells transfected with the control scrambled oligomer. On the other hand, cotransfection with pre-miR-29b and the *uc.173* expression vector did not alter the expression levels of occludin or E-cadherin protein. Taken together, these findings indicate that increasing *uc.173* levels stimulates claudin-1 translation and enhances the barrier function, largely through the action of *uc.173* as a molecular sponge for miR-29b to reduce its bioavailability to *CLDN1* mRNA.

DISCUSSION

Claudin-1 is a member of the claudin family of TJs. Claudins seal epithelial cells together in the intestinal epithelium in a way that prevents even small molecules from leaking between cells (1, 36), but the exact mechanisms that control cellular claudin-1 abundance are largely unknown. In this study, we show that the T-UCR *uc.173* is a novel regulator of claudin-1 expression and that increasing the levels of *uc.173* stimulates claudin-1 translation without affecting total *CLDN1* mRNA levels. As shown above, *uc.173* did not bind to *CLDN1* mRNA but acted as a decoy RNA for miR-29b, which represses claudin-1 translation via direct interaction with the *CLDN1* 3′ UTR. The present study also highlights the importance of *uc.173*-mediated claudin-1 expression in the regulation of gut permeability, since decreased levels of claudin-1 due to *uc.173* silencing not only resulted in epithelial barrier dysfunction *in vitro* but also increased the vulnerability of the gut barrier to septic stress in mice. Because of the striking evolutionary retention of T-UCRs in the human genome, these findings provide a strong rationale and a fundamental basis for developing new therapeutic strategies directed at *uc.173* and/or its target, miR-29b, in order to preserve the integrity of gut barrier function in stressful environments, especially in surgical intensive care patients supported with total parenteral nutrition.

T-UCRs are highly expressed in the epithelium of the intestinal mucosa, and their levels change remarkably after food starvation, during inflammation, and in cancers (23, 29, 37). T-UCR expression profiles are also dysregulated in human Barrett's esophagus (38). However, our understanding of the biological functions of T-UCRs and their involvement in pathology in the gut mucosa is limited. Our present results constitute the first demonstration that *uc.173* is essential for maintaining the normal function of the intestinal epithelial barrier by enhancing claudin-1 expression. In cultured IECs, *uc.173* silencing specifically decreased the levels of cellular claudin-1 protein, since it did not affect the expression levels of other TJs, such as claudin-3, occludin, JAM-1, and ZO-1, nor that of the AJ E-cadherin. Decreased levels of claudin-1 in *uc.173*-silenced cells were associated with epithelial barrier dysfunction in an *in vitro* model. In keeping with these results, the degree of CLP-induced gut permeability in mice treated with LNA-modified anti-uc.173 was much higher than that observed in mice treated with a control oligomer. Moreover, ectopically expressed *uc.173* enhanced nascent claudin-1 protein synthesis and increased the levels of *CLDN1* mRNA associated with actively translating fractions of polyribosomes. In support of our present findings, *uc.173* enhances the growth of the small intestinal mucosa in mice (29) and inhibits lead-induced neuronal apoptosis in brain tissue (39). In contrast, the T-UCR *uc.261* was found to decrease TJ expression and repress TJ assembly, thus damaging intestinal epithelial barrier function (37). Clearly, more studies are needed to fully investigate the exact roles and mechanisms of different T-UCRs in the regulation of epithelial barrier function under various pathophysiological conditions.

In this study, we also observed that *uc.173* interacted directly with miR-29b via the complementary sites located at its 3′ end, suggesting the possibility that *uc.173* can act as a molecular sponge for miR-29b so as to reduce the availability of miR-29b to *CLDN1* mRNA. As shown in Fig. S2 in the supplemental material, MS2-tagged *uc.173* specifically pulled down miR-29b in IECs but did not bind to miR-222 or lncRNA *H19*. Furthermore, miR-29b was associated only with *uc.173*, not with *uc.346* or *uc.283*, as measured by RNA pulldown assays using biotin-labeled miR-29b (Fig. 5C). In keeping with our present results, several T-UCRs have been shown to regulate gene expression by

interacting with given miRNAs but not directly targeting mRNAs (23). For example, *uc.339* functions as a natural decoy RNA for three miRNAs—miR-339-3p, miR-663-3p, and miR-95-5p—in lung cancer cells (26), while *uc.8+* entraps miR-596 and reduces the availability of this miRNA to *MMP9* mRNA in bladder tissues (25). In addition, T-UCRs can also regulate miRNA activity at another level. It has been reported that *uc.283+* controls miRNA processing by preventing pri-miRNA cleavage by Drosha (17). We have recently demonstrated that *uc.173* interferes with miRNA stability by binding to pri-miR-195 via sequence complementarity in IECs (29). It is likely that *uc.173* affects gene regulatory programs governing intestinal epithelial homeostasis and barrier function predominantly by functioning as a decoy RNA, as for miR-29b, and/or by modulating miRNA degradation, as for miR-195.

Our present results also indicate that miR-29b represses claudin-1 translation by interacting directly with the 3′ UTR of *CLDN1* mRNA, but not with its 5′ UTR or CR, in IECs. Studies using various ectopic luciferase reporters bearing partial transcripts spanning the *CLDN1* 3′ UTR with or without the miR-29b binding site further show that a specific sequence at positions 2129 to 2151 in 3′-UTR-F3 was the predominant functional site through which miR-29b interacted with claudin-1 and repressed its translation, whereas another predicted site, located in 3′-UTR-F4, exhibited a lesser effect. These findings are consistent with results from others, who demonstrate that miR-29b commonly interacts with the 3′ UTRs of its target transcripts, such as *bcr-abl1*, *gata3*, *pdpn*, *col1a1*, *col3a1*, *col5a1*, *eln*, *Cdk2*, *dnmt3a*, and *dnmt3b* mRNAs, thus destabilizing mRNAs and/or repressing their translation (20, 33, 40–44). In some instances, miR-29b also binds to the CRs of target mRNAs for its regulatory actions. For example, miR-29b destabilizes *Men1* mRNA through a single binding site in the CR of *Men1* mRNA rather than in its 3′ UTR (34). In a similar manner, miR-322/503 represses *Smurf2* mRNA translation by interacting with the *Smurf2* CR (45), and miR-222 inhibits *Cdk4* mRNA translation through interaction with the *Cdk4* CR (46).

Finally, our findings show that increasing *uc.173* levels in cells overexpressing miR-29b rescued claudin-1 expression and restored epithelial barrier function by reducing the association of miR-29b with *CLDN1* mRNA. miR-29b is a potent repressor of intestinal mucosal regeneration, and elevation of cellular miR-29b levels causes mucosal atrophy and compromises the integrity of the intestinal epithelium in mice (20, 33, 35). Our present studies provide additional evidence that *uc.173*-mediated repression of miR-29b also contributes to the stimulation of intestinal mucosal growth after *uc.173* overexpression. On the other hand, miR-195 represses IEC migration over the wounded area after injury by targeting *Stim1* mRNA, thus impairing the repair of the intestinal epithelium (47). Therefore, inhibition of miR-195 activity by *uc.173* (29) also plays a role in the *uc.173*-mediated protective effect on the epithelial barrier. Because the basal level of mucosal *uc.173* is relatively high in the intestine and its levels in tissue decrease dramatically in stressful environments, enhancement of epithelial barrier function and mucosal regeneration by *uc.173* through antagonism of miR-29b and miR-195 is crucial for homeostasis of the intestinal epithelium, representing a novel therapeutic target for patients with gut barrier dysfunction and mucosal atrophy or hyperplasia.

MATERIALS AND METHODS

Cell culture and animals. Caco-2 cells were purchased from the American Type Culture Collection (Manassas, VA) and were maintained under standard culture conditions (48). Tissue culture medium and fetal bovine serum were purchased from Invitrogen (Carlsbad, CA), and biochemicals were from Sigma (St. Louis, MO). The antibodies recognizing claudin-1, claudin-3, occludin, JAM-1, ZO-1, E-cadherin, β-catenin, UBE2B, and GAPDH were obtained from Santa Cruz Biotechnology (Santa Cruz, CA) and BD Biosciences (Sparks, MD). The secondary antibody conjugated to horseradish peroxidase was from Sigma. LNA-modified anti-uc.173 oligonucleotides and control LNA-scrambled oligonucleotides were custom-generated by Exiqon (Vedbæk, Denmark). The pre-miR miRNA precursor of miRNA-29b (pre-miR-195) was purchased from Ambion (Austin, TX). Biotin-labeled miRNA-29b was custom-made by Dharmacon (Lafayette, CO).

C57BL/6J mice (male and female, 6 to 9 weeks old) were purchased from The Jackson Laboratory (Bar Harbor, ME) and were housed in a pathogen-free animal facility at the Baltimore VA Medical Center. All animal experiments were conducted in accordance with NIH guidelines and were approved by the Institutional Animal Care and Use Committee of the University of Maryland School of Medicine and the

Baltimore VA hospital. In studies of LNA-mediated *uc.173* silencing, mice were injected intraperitoneally (i.p.) with LNA–anti-uc.173 (500 μg/100 g of body weight/day) for 4 consecutive days, whereas control mice were injected with an equal dose of control LNA-scrambled oligonucleotides as described previously (29). On day 5, a 4-cm segment taken from the middle of the small intestine was removed, and the mucosa was scraped with a glass slide for various measurements.

Plasmid construction. An expression vector containing a 284-bp fragment flanking the human *uc.173* locus under the control of the pCMV promoter was constructed as described previously (29). The chimeric firefly luciferase reporter constructs containing the full-length *CLDN1* 5′ UTR, CR, or different 3′ UTR fragments were subcloned into the Dual-Luciferase miRNA target expression vector pmirGLO (Promega, Madison, WI) to generate pmirGLO-Luc-CLDN1-5′UTR, pmirGLO-Luc-CLDN1-CR, and pmirGLO-CLDN1-3′UTR as described previously (49). DNA sequencing and enzyme digestion were used to confirm the sequence and orientation of the fragment in the luciferase reporter. Transient transfections were performed using the Lipofectamine reagent as recommended by the manufacturer (Invitrogen) (30). Luciferase activity was examined using the Dual-Luciferase assay system, and the levels of firefly luciferase activity were normalized to the levels of *Renilla* luciferase activity and were further compared with the levels of luciferase mRNA in every experiment. All the primer sequences used to generate these constructs are given in Table S1 in the supplemental material. Both the pcDNA-MS2 and pcDNA-MS2-GST plasmids have been described previously (32), and full-length *uc.173* was inserted into pcDNA-MS2 at the XhoI site as described previously (7, 47).

RT-PCR and Q-PCR analysis. Total RNA was isolated by using an RNeasy minikit (Qiagen, Valencia, CA), and reverse transcription (RT) and PCR amplification reactions were performed as described previously (50). The levels of the *GAPDH* PCR product were examined to monitor the evenness of RNA input in RT-PCR samples. Real-time quantitative PCR (Q-PCR) analysis was conducted using 7500 Fast Real-Time PCR systems with specific primers, probes, and software (Applied Biosystems, Foster City, CA). For miRNA studies, the levels of miRNA-29b were also quantified by Q-PCR by using a TaqMan microRNA assay; the small nuclear RNA (snRNA) *U6* was used as an endogenous control.

Western blot analysis. Whole-cell lysates were prepared using 2% SDS, sonicated, and centrifuged (12,000 rpm) at 4°C for 15 min. The supernatants were boiled for 5 min and were size-fractionated by SDS-PAGE (7.5% acrylamide). After proteins were transferred to nitrocellulose filters, the blots were incubated with primary antibodies recognizing claudin-1 or other TJs; following incubations with secondary antibodies, immunocomplexes were developed by using chemiluminescence.

Analysis of newly translated protein. *De novo* synthesis of nascent proteins was detected by a Click-iT protein analysis detection kit (Life Technologies, Grand Island, NY) according to the manufacturer's instructions, with minor modifications as described previously (18). Briefly, cells were first incubated in a methionine-free medium and then exposed to L-azidohomoalanine (AHA). After the cell lysates were mixed with the reaction buffer containing a biotin-alkyne reagent and $CuSO_4$ for 20 min, the biotin-alkyne-azide-modified protein complex was pulled down using paramagnetic streptavidin-conjugated Dynabeads. The pulldown material was resolved by 10% SDS-PAGE and was analyzed by Western immunoblot analysis using antibodies that recognized claudin-1 or GAPDH protein.

Polysome analysis was performed as described previously (51). Briefly, cells at ~70% confluence were incubated for 15 min in 0.1 mg/ml cycloheximide, lifted by scraping in 1 ml of polysome extraction buffer, and lysed on ice for 10 min. Nuclei were pelleted, and the resulting supernatant was fractionated through a 10-to-50% linear sucrose gradient to fractionate cytoplasmic components according to their molecular weights. Fractions were eluted with a fraction collector (Brandel, Gaithersburg, MD), and their quality was monitored at 254 nm using a UV-6 detector (ISCO, Louisville, KY). After the RNA in each fraction was extracted, the level of each individual mRNA was quantified by Q-PCR in each of the fractions.

Biotin-labeled RNA pulldown assays. Biotin-labeled pri-miR-29b was transfected, and 24 h later, whole-cell lysates were collected, mixed with streptavidin-coupled Dynal beads, and incubated on a rotator overnight (52). After the beads were washed thoroughly, the bead-bound RNA was isolated and subjected to RT, followed by Q-PCR analysis. Input RNA was extracted and served as a control.

Measurements of epithelial barrier function *in vitro*. Epithelial barrier function *in vitro* was examined by paracellular tracer flux assays using the 12-well Transwell plate (surface area, 1.12 cm^2) as described previously (19). FITC-dextran (70 kDa; Sigma), a membrane-impermeant molecule, served as the paracellular tracer and was added to the apical bathing wells. The basal bathing well had no added tracers and contained the same flux assay medium as that in the apical compartment. All flux assays were performed at 37°C, and the basal medium was collected at different times after the addition of FITC-dextran. The concentration of FITC-dextran in the basal medium was determined using a fluorescence plate reader with an excitation wavelength of 490 nm and an emission wavelength of 530 nm. TEER was measured with an epithelial volt/ohm meter under open-circuit conditions (World Precision Instruments, Sarasota, FL) as described previously (53), and the TEER values of all monolayers were normalized to those of control monolayers in the same experiment.

Surgical procedures. Mice were anesthetized with pentobarbital (Nembutal; 5.5 mg/100 g of body weight, given i.p.), and CLP was performed as described previously (31). The distal portion of the cecum (1 cm) was ligated with 5-0 silk sutures. The ligated cecum was then punctured with a 25-gauge needle and was slightly compressed with an applicator until a small amount of stool appeared. In sham-operated animals, the cecum was manipulated, but without ligation and puncture, and was placed back in the peritoneum. The incision was closed using a 2-layer procedure: 5-0 silk sutures on the muscle layer and the skin, respectively. Mice received 1 ml of saline i.p. for fluid resuscitation at the time of closure

and 0.1 mg buprenorphine (Buprenex)/100 g of body weight subcutaneously (s.c.) 4 times at 12-h intervals to minimize distress.

Gut permeability *in vivo* was determined by examining the appearance in blood of FITC-dextran administered by gavage as described previously (54). Briefly, mice were gavaged with FITC-dextran at a dose of 60 mg/100 g of body weight 4 h before harvest. Blood samples were collected by cardiac puncture. The concentration of FITC-dextran in serum was determined using a fluorescence plate reader as described above.

Statistical analysis. All values are expressed as means ± standard errors of the means (SEM). An unpaired, two-tailed Student *t* test was used where indicated, and a *P* value of <0.05 was considered significant. In assessing multiple groups, one-way analysis of variance (ANOVA) was utilized with Tukey's *post hoc* test (55). The statistical software used was SPSS 17.1.

SUPPLEMENTAL MATERIAL

Supplemental material for this article may be found at https://doi.org/10.1128/MCB.00010-18.

SUPPLEMENTAL FILE 1, PDF file, 0.1 MB.

ACKNOWLEDGMENTS

This work was supported by Merit Review Awards (to Jian-Ying Wang and J. N. Rao) from the U.S. Department of Veterans Affairs, grants from the National Institutes of Health (DK57819, DK61972, and DK68491, to Jian-Ying Wang), and funding from the National Institute on Aging Intramural Research Program, NIH (to M. Gorospe). Jian-Ying Wang is a Senior Research Career Scientist, Biomedical Laboratory Research & Development Service, U.S. Department of Veterans Affairs.

Jun-Yao Wang and Y.-H. Cui performed most experiments and summarized the data. L. Xiao and H. K. Chung performed *in vivo* experiments and biotin pulldown assays. Y. Zhang and J. N. Rao performed experiments with the miR-29b promoter. M. Gorospe contributed to the experimental design and data analysis. Jian-Ying Wang designed the experiments, analyzed the data, prepared figures, and drafted the manuscript.

We declare that we have no competing interests.

REFERENCES

1. Turner JR. 2009. Intestinal mucosal barrier function in health and disease. Nat Rev Immunol 9:799–809. https://doi.org/10.1038/nri2653.
2. Yang H, Rao JN, Wang JY. 2014. Posttranscriptional regulation of intestinal epithelial tight junction barrier by RNA-binding proteins and microRNAs. Tissue Barriers 2:e28320. https://doi.org/10.4161/tisb.28320.
3. Higashi T, Miller AL. 2017. Tricellular junctions: how to build junctions at the TRICkiest points of epithelial cells. Mol Biol Cell 28:2023–2034. https://doi.org/10.1091/mbc.E16-10-0697.
4. Furuse M, Izumi Y, Oda Y, Higashi T, Iwamoto N. 2014. Molecular organization of tricellular tight junctions. Tissue Barriers 2:e28960. https://doi.org/10.4161/tisb.28960.
5. Malinova TS, Huveneers S. 2018. Sensing of cytoskeletal forces by asymmetric adherens junctions. Trends Cell Biol 28:328–341. https://doi.org/10.1016/j.tcb.2017.11.002.
6. Chen J, Xiao L, Rao JN, Zou T, Liu L, Bellavance E, Gorospe M, Wang JY. 2008. JunD represses transcription and translation of the tight junction protein zona occludens-1 modulating intestinal epithelial barrier function. Mol Biol Cell 19:3701–3712. https://doi.org/10.1091/mbc.E08-02-0175.
7. Yu TX, Wang PY, Rao JN, Zou T, Liu L, Xiao L, Gorospe M, Wang JY. 2011. Chk2-dependent HuR phosphorylation regulates occludin mRNA translation and epithelial barrier function. Nucleic Acids Res 39:8472–8487. https://doi.org/10.1093/nar/gkr567.
8. Bhatt T, Rizvi A, Batta SP, Kataria S, Jamora C. 2013. Signaling and mechanical roles of E-cadherin. Cell Commun Adhes 20:189–199. https://doi.org/10.3109/15419061.2013.854778.
9. Carter SR, Zahs A, Palmer JL, Wang L, Ramirez L, Gamelli RL, Kovacs EJ. 2013. Intestinal barrier disruption as a cause of mortality in combined radiation and burn injury. Shock 40:281–289. https://doi.org/10.1097/SHK.0b013e3182a2c5b5.
10. Wang KC, Chang HY. 2011. Molecular mechanisms of long noncoding RNAs. Mol Cell 43:904–914. https://doi.org/10.1016/j.molcel.2011.08.018.
11. Ulitsky I, Bartel DP. 2013. lincRNAs: genomics, evolution, and mechanisms. Cell 154:26–46. https://doi.org/10.1016/j.cell.2013.06.020.
12. Batista PJ, Chang HY. 2013. Long noncoding RNAs: cellular address codes in development and disease. Cell 152:1298–1307. https://doi.org/10.1016/j.cell.2013.02.012.
13. Esteller M. 2011. Non-coding RNAs in human disease. Nat Rev Genet 12:861–874. https://doi.org/10.1038/nrg3074.
14. Ørom UA, Derrien T, Beringer M, Gumireddy K, Gardini A, Bussotti G, Lai F, Zytnicki M, Notredame C, Huang Q, Guigo R, Shiekhattar R. 2010. Long noncoding RNAs with enhancer-like function in human cells. Cell 143:46–58. https://doi.org/10.1016/j.cell.2010.09.001.
15. Keniry A, Oxley D, Monnier P, Kyba M, Dandolo L, Smits G, Reik W. 2012. The *H19* lincRNA is a developmental reservoir of miR-675 that suppresses growth and *Igf1r*. Nat Cell Biol 14:659–665. https://doi.org/10.1038/ncb2521.
16. Gao Y, Wu F, Zhou J, Yan L, Jurczak MJ, Lee HY, Yang L, Mueller M, Zhou XB, Dandolo L, Szendroedi J, Roden M, Flannery C, Taylor H, Carmichael GG, Shulman GI, Huang Y. 2014. The *H19*/let-7 double-negative feedback loop contributes to glucose metabolism in muscle cells. Nucleic Acids Res 42:13799–13811. https://doi.org/10.1093/nar/gku1160.
17. Liz J, Portela A, Soler M, Gómez A, Ling H, Michlewski G, Calin GA, Guil S, Esteller M. 2014. Regulation of pri-miRNA processing by a long noncoding RNA transcribed from an ultraconserved region. Mol Cell 55:138–147. https://doi.org/10.1016/j.molcel.2014.05.005.
18. Zou T, Jaladanki SK, Liu L, Xiao L, Chung HK, Wang JY, Xu Y, Gorospe M, Wang JY. 2016. *H19* long noncoding RNA regulates intestinal epithelial barrier function via microRNA 675 by interacting with RNA-binding protein HuR. Mol Cell Biol 36:1332–1341. https://doi.org/10.1128/MCB.01030-15.
19. Xiao L, Rao JN, Cao S, Liu L, Chung HK, Zhang Y, Zhang J, Liu Y, Gorospe

M, Wang JY. 2016. Long noncoding RNA *SPRY4-IT1* regulates intestinal epithelial barrier function by modulating the expression levels of tight junction proteins. Mol Biol Cell 27:617–626. https://doi.org/10.1091/mbc.E15-10-0703.
20. Wang JY, Xiao L, Wang JY. 2017. Posttranscriptional regulation of intestinal epithelial integrity by noncoding RNAs. Wiley Interdiscip Rev RNA 8:1399. https://doi.org/10.1002/wrna.1399.
21. Bejerano G, Pheasant M, Makunin I, Stephen S, Kent WJ, Mattick JS, Haussler D. 2004. Ultraconserved elements in the human genome. Science 304:1321–1325. https://doi.org/10.1126/science.1098119.
22. Calin GA, Liu CG, Ferracin M, Hyslop T, Spizzo R, Sevignani C, Fabbri M, Cimmino A, Lee EJ, Wojcik SE, Shimizu M, Tili E, Rossi S, Taccioli C, Pichiorri F, Liu X, Zupo S, Herlea V, Gramantieri L, Lanza G, Alder H, Rassenti L, Volinia S, Schmittgen TD, Kipps TJ, Negrini M, Croce CM. 2007. Ultraconserved regions encoding ncRNAs are altered in human leukemias and carcinomas. Cancer Cell 12:215–229. https://doi.org/10.1016/j.ccr.2007.07.027.
23. Ling H, Vincent K, Pichler M, Fodde R, Berindan-Neagoe I, Slack FJ, Calin GA. 2015. Junk DNA and the long non-coding RNA twist in cancer genetics. Oncogene 34:5003–5011. https://doi.org/10.1038/onc.2014.456.
24. Braconi C, Valeri N, Kogure T, Gasparini P, Huang N, Nuovo GJ, Terracciano L, Croce CM, Patel T. 2011. Expression and functional role of a transcribed noncoding RNA with an ultraconserved element in hepatocellular carcinoma. Proc Natl Acad Sci U S A 108:786–791. https://doi.org/10.1073/pnas.1011098108.
25. Olivieri M, Ferro M, Terreri S, Durso M, Romanelli A, Avitabile C, De Cobelli O, Messere A, Bruzzese D, Vannini I, Marinelli L, Novellino E, Zhang W, Incoronato M, Ilardi G, Staibano S, Marra L, Franco R, Perdonà S, Terracciano D, Czerniak B, Liguori GL, Colonna V, Fabbri M, Febbraio F, Calin GA, Cimmino A. 2016. Long noncoding RNA containing ultraconserved genomic region 8 promotes bladder cancer tumorigenesis. Oncotarget 7:20636–20654. https://doi.org/10.18632/oncotarget.7833.
26. Vannini I, Wise PM, Challagundla KB, Plousiou M, Raffini M, Bandini E, Fanini F, Paliaga G, Crawford M, Ferracin M, Ivan C, Fabris L, Davuluri RV, Guo Z, Cortez MA, Zhang X, Chen L, Zhang S, Fernandez-Cymering C, Han L, Carloni S, Salvi S, Ling H, Murtadha M, Neviani P, Gitlitz BJ, Laird-Offringa IA, Nana-Sinkam P, Negrini M, Liang H, Amadori D, Cimmino A, Fabbri M, Calin GA. 2017. Transcribed ultraconserved region 339 promotes carcinogenesis by modulating tumor suppressor microRNAs. Nat Commun 8:1801. https://doi.org/10.1038/s41467-017-01562-9.
27. Sekino Y, Sakamoto N, Goto K, Honma R, Shigematsu Y, Sentani K, Oue N, Teishima J, Matsubara A, Yasui W. 2017. Transcribed ultraconserved region Uc.63+ promotes resistance to docetaxel through regulation of androgen receptor signaling in prostate cancer. Oncotarget 8:94259–94270. https://doi.org/10.18632/oncotarget.21688.
28. Ferdin J, Nishida N, Wu X, Nicoloso MS, Shah MY, Devlin C, Ling H, Shimizu M, Kumar K, Cortez MA, Ferracin M, Bi Y, Yang D, Czerniak B, Zhang W, Schmittgen TD, Voorhoeve MP, Reginato MJ, Negrini M, Davuluri RV, Kunej T, Ivan M, Calin GA. 2013. HINCUTs in cancer: hypoxia-induced noncoding ultraconserved transcripts. Cell Death Differ 20:1675–1687. https://doi.org/10.1038/cdd.2013.119.
29. Xiao L, Wu J, Wang JY, Chung HK, Kalakonda S, Rao JN, Gorospe M, Wang JY. 2018. Long noncoding RNA *uc.173* promotes renewal of the intestinal mucosa by inducing degradation of microRNA 195. Gastroenterology 154:599–611. https://doi.org/10.1053/j.gastro.2017.10.009.
30. Liu L, Ouyang M, Rao JN, Zou T, Xiao L, Chung HK, Wu J, Donahue JM, Gorospe M, Wang JY. 2015. Competition between RNA-binding proteins CELF1 and HuR modulates MYC translation and intestinal epithelium renewal. Mol Biol Cell 26:1797–1810. https://doi.org/10.1091/mbc.E14-11-1500.
31. Hubbard WJ, Choudhry M, Schwacha MG, Kerby JD, Rue LW, III, Bland KI, Chaudry IH. 2005. Cecal ligation and puncture. Shock 1:52–57. https://doi.org/10.1097/01.shk.0000191414.94461.7e.
32. Yoon JH, Srikantan S, Gorospe M. 2012. MS2-TRAP (MS2-tagged RNA affinity purification): tagging RNA to identify associated miRNAs. Methods 58:81–87. https://doi.org/10.1016/j.ymeth.2012.07.004.
33. Xiao L, Rao JN, Zou T, Liu L, Cao S, Martindale JL, Su W, Chung HK, Gorospe M, Wang JY. 2013. miR-29b represses intestinal mucosal growth by inhibiting translation of cyclin-dependent kinase 2. Mol Biol Cell 24:3038–3046. https://doi.org/10.1091/mbc.E13-05-0287.
34. Ouyang M, Su W, Xiao L, Rao JN, Jiang L, Li Y, Turner DJ, Gorospe M, Wang JY. 2015. Modulation by miR-29b of intestinal epithelium homoeostasis through the repression of menin translation. Biochem J 465:315–323. https://doi.org/10.1042/BJ20141028.
35. Li Y, Chen G, Wang J, Zou T, Liu L, Xiao L, Chung HK, Rao JN, Wang JY. 2016. Posttranscriptional regulation of Wnt-coreceptor LRP6 and RNA-binding protein HuR by miR-29b in intestinal epithelial cells. Biochem J 473:1641–1649. https://doi.org/10.1042/BCJ20160057.
36. Schneeberger EE, Lynch RD. 2004. The tight junction: a multifunctional complex. Am J Physiol Cell Physiol 286:C1213–C1228. https://doi.org/10.1152/ajpcell.00558.2003.
37. Qian XX, Peng JC, Xu AT, Zhao D, Qiao YQ, Wang TR, Shen J, Ran ZH. 2016. Noncoding transcribed ultraconserved region (T-UCR) *uc.261* participates in intestinal mucosa barrier damage in Crohn's disease. Inflamm Bowel Dis 22:2840–2852. https://doi.org/10.1097/MIB.0000000000000945.
38. Fassan M, Dall'Olmo L, Galasso M, Braconi C, Pizzi M, Realdon S, Volinia S, Valeri N, Gasparini P, Baffa R, Souza RF, Vicentini C, D'Angelo E, Bornschein J, Nuovo GJ, Zaninotto G, Croce CM, Rugge M. 2014. Transcribed ultraconserved noncoding RNAs (T-UCR) are involved in Barrett's esophagus carcinogenesis. Oncotarget 5:7162–7171. https://doi.org/10.18632/oncotarget.2249.
39. Nan A, Zhou X, Chen L, Liu M, Zhang N, Zhang L, Luo Y, Liu Z, Dai L, Jiang Y. 2016. A transcribed ultraconserved noncoding RNA *uc.173* is a key molecule for the inhibition of lead-induced neuronal apoptosis. Oncotarget 7:112–124. https://doi.org/10.18632/oncotarget.6590.
40. Cortez MA, Nicoloso MS, Shimizu M, Rossi S, Gopisetty G, Molina JR, Carlotti C, Jr, Tirapelli D, Neder L, Brassesco MS, Scrideli CA, Tone LG, Georgescu MM, Zhang W, Puduvalli V, Calin GA. 2010. miR-29b and miR-125a regulate podoplanin and suppress invasion in glioblastoma. Genes Chromosomes Cancer 49:981–990. https://doi.org/10.1002/gcc.20808.
41. Huang X, Schwind S, Yu B, Santhanam R, Wang H, Hoellerbauer P, Mims A, Klisovic R, Walker AR, Chan KK, Blum W, Perrotti D, Byrd JC, Bloomfield CD, Caligiuri MA, Lee RJ, Garzon R, Muthusamy N, Lee LJ, Marcucci G. 2013. Targeted delivery of microRNA-29b by transferrin-conjugated anionic lipopolyplex nanoparticles: a novel therapeutic strategy in acute myeloid leukemia. Clin Cancer Res 19:2355–2367. https://doi.org/10.1158/1078-0432.CCR-12-3191.
42. Melo SA, Kalluri R. 2013. miR-29b moulds the tumour microenvironment to repress metastasis. Nat Cell Biol 15:139–140. https://doi.org/10.1038/ncb2684.
43. Qin W, Chung AC, Huang XR, Meng XM, Hui DS, Yu CM, Sung JJ, Lan HY. 2011. TGF-β/Smad3 signaling promotes renal fibrosis by inhibiting miR-29. J Am Soc Nephrol 22:1462–1474. https://doi.org/10.1681/ASN.2010121308.
44. Roderburg C, Urban GW, Bettermann K, Vucur M, Zimmermann H, Schmidt S, Janssen J, Koppe C, Knolle P, Castoldi M, Tacke F, Trautwein C, Luedde T. 2011. MicroRNA profiling reveals a role for miR-29 in human and murine liver fibrosis. Hepatology 53:209–218. https://doi.org/10.1002/hep.23922.
45. Cao S, Xiao L, Rao JN, Zou T, Liu L, Zhang D, Turner DJ, Gorospe M, Wang JY. 2014. Inhibition of Smurf2 translation by miR-322/503 modulates TGF-β/Smad2 signaling and intestinal epithelial homeostasis. Mol Biol Cell 25:1234–1243. https://doi.org/10.1091/mbc.E13-09-0560.
46. Xiao L, Cui YH, Rao JN, Zou T, Liu L, Smith A, Turner DJ, Gorospe M, Wang JY. 2011. Regulation of cyclin-dependent kinase 4 translation through CUG-binding protein 1 and microRNA-222 by polyamines. Mol Biol Cell 22:3055–3069. https://doi.org/10.1091/mbc.E11-01-0069.
47. Zhuang R, Rao JN, Zou T, Liu L, Xiao L, Cao S, Hansraj NZ, Gorospe M, Wang JY. 2013. miR-195 competes with HuR to modulate stim1 mRNA stability and regulate cell migration. Nucleic Acids Res 41:7905–7919. https://doi.org/10.1093/nar/gkt565.
48. Cui YH, Xiao L, Rao JN, Zou T, Liu L, Chen Y, Turner DJ, Gorospe M, Wang JY. 2012. miR-503 represses CUG-binding protein 1 translation by recruiting CUGBP1 mRNA to processing bodies. Mol Biol Cell 23:151–162. https://doi.org/10.1091/mbc.E11-05-0456.
49. Zhang Y, Zhang Y, Xiao L, Yu TX, Li JZ, Rao JN, Turner DJ, Gorospe M, Wang JY. 2017. Cooperative repression of insulin-like growth factor type 2 receptor translation by microRNA 195 and RNA-binding protein CUGBP1. Mol Cell Biol 37:e00225-17. https://doi.org/10.1128/MCB.00225-17.
50. Liu L, Christodoulou-Vafeiadou E, Rao JN, Zou T, Xiao L, Chung HK, Yang H, Gorospe M, Kontoyiannis D, Wang JY. 2014. RNA-binding protein HuR promotes growth of small intestinal mucosa by activating the Wnt signaling pathway. Mol Biol Cell 25:3308–3318. https://doi.org/10.1091/mbc.E14-03-0853.
51. Liu L, Zhuang R, Xiao L, Chung HK, Luo J, Turner DJ, Rao JN, Gorospe M, Wang JY. 2017. HuR enhances early restitution of the intestinal epithe-

lium by increasing Cdc42 translation. Mol Cell Biol 37:e00574-16. https://doi.org/10.1128/MCB.00574-16.
52. Chung HK, Chen Y, Rao JN, Liu L, Xiao L, Turner DJ, Yang P, Gorospe M, Wang JY. 2015. Transgenic expression of miR-222 disrupts intestinal epithelial regeneration by targeting multiple genes including Frizzled-7. Mol Med 21:676–687. https://doi.org/10.2119/molmed.2015.00147.
53. Yu TX, Rao JN, Zou T, Liu L, Xiao L, Ouyang M, Cao S, Gorospe M, Wang JY. 2013. Competitive binding of CUGBP1 and HuR to occludin mRNA controls its translation and modulates epithelial barrier function. Mol Biol Cell 24:85–99. https://doi.org/10.1091/mbc.E12-07-0531.
54. Furuta GT, Turner JR, Taylor CT, Hershberg RM, Comerford K, Narravula S, Podolsky DK, Colgan SP. 2001. Hypoxia-inducible factor 1-dependent induction of intestinal trefoil factor protects barrier function during hypoxia. J Exp Med 193:1027–1034. https://doi.org/10.1084/jem.193.9.1027.
55. Harter JL. 1960. Critical values for Duncan's new multiple range tests. Biometrics 16:671–685. https://doi.org/10.2307/2527770.